AIChE WILEY InterScience DISCOVER SOMETHING GREAT

R&D NOTES

CFD Simulations for Analysis and Scale-up of Anti-Solvent Crystallization

Xiaomin Liu, Dimitri Hatziavramidis, Hamid Arastoopour, and Allan S. Myerson
Particle Technology and Crystallization Center, Dept. of Chemical & Environmental Engineering, Illinois Institute of Technology, Chicago, IL 60616

DOI 10.1002/aic.10962
Published online August 29, 2006 in Wiley InterScience (www.interscience.wiley.com).

Keywords: crystallization, design of experiments, computational fluid dynamics, mixing, scale-up

Introduction

Crystallization from solution is commonly used in the pharmaceutical industry as the final step in the production of active pharmaceutical ingredients (API). One of the most common methods of supersaturation generation is through the addition of an antisolvent (which reduces solute solubility), which is often used in combination with cooling to maximize yield and to produce crystals of desired quality in terms of purity, size, morphology, and shape.[1,2] API with large crystal size and a narrow crystal-size distribution (CSD) are often preferred, because of advantages in downstream operations such as filtration, drying, size reduction and, eventually, formulation into tablets or capsules. Nucleation and growth kinetics, and supersaturation are the primary factors affecting CSD. Mixing is known to have a significant effect on supersaturation distribution, nucleation kinetics and final product-size distribution. In batch crystallization, mixing similarity is important in scale-up[1] from laboratory scale, where it is common to determine nucleation and crystallization kinetics, to full industrial scale, where actual production takes place.

In most scale-up cases, as a result of conflicting requirements,[3,4] it is impossible to achieve simultaneously geometric, dynamic and kinematic similarity. Successful scale-up begins by identifying mixing requirements and critical mechanisms.[5] Mixing requirements for antisolvent crystallization apply to blending of solution and antisolvent, and solid-liquid mixing,[6] where the liquid is a mixture of primary solvent and antisolvent. Mixing occurs at three levels; (1) micromixing, at molecular scales, (2) mesomixing, at scales comparable to the extent of segregated fluid, and (3) macromixing, at scales comparable to the size of the crystallizer[1,7] There are several well-known scale-up criteria,[3] for example, constant power input per unit volume, and constant impeller tip speed. The former ensures the same local energy dissipation and is more relevant to micromixing; the latter is more relevant to mesomixing.

In order to achieve good-quality crystals in antisolvent crystallization, care must be taken to suppress the sharp gradients in antisolvent concentration. The sharp concentration fronts generated by antisolvent addition prolong nucleation at the expense of crystal growth and result in poor-quality crystals.[1] A scale-up rule is needed to achieve similarity in macromixing and blending of antisolvent and solution.

In recent years, the influence of mixing on processes has been studied by CFD simulations.[8-12] Wei[13] reported on the transient supersaturation distribution in a 3-D stirred vessel, and the effects of feed locations and impeller speed on mixing and CSD in precipitation. His simulations showed the existence of a high-supersaturation zone and the production of a larger number of crystals than a perfectly mixed model predicted. Experimental studies[14,15,16] have reported the effects of the impeller speed, reactant feed location, and feed rate on mixing and CSD. Guidelines of feed strategies have also been discussed in books on crystallization.[1]

This article presents a study of mixing of solvent and antisolvent that can be described by single-phase flow, before a significant number of crystals of size sufficient to warrant two-phase flow description (particle Stokes number exceeds unity) forms. A similar study of mixing in a liquid-solid system after crystallization progresses will follow. The article utilizes CFD numerical experiments, designed by DOE methodologies to determine: (1) the effects of agitation rate, and antisolvent feed rate and position on mixing (screening DOE), and (2) the appropriate parameters for mixing in scale-up from laboratory to full industrial scale vessels (optimization DOE).

CFD Simulations

Physical and computational model

The system of interest is anti-solvent crystallization of glycine from a water-ethanol mixture at 25°C, where ethanol is the antisolvent, continuously fed to the crystallizer.

Correspondence concerning this article should be addressed to D. Hatziavramidis at Hatziavramidis@iit.edu.

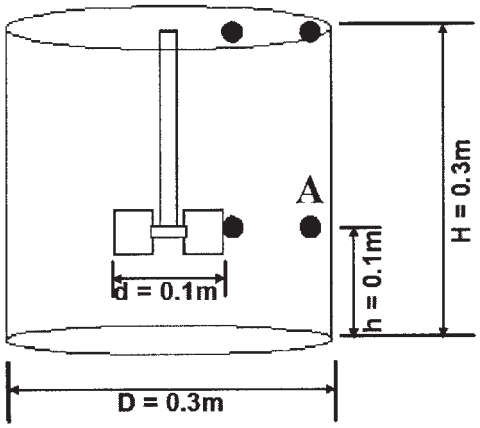

Figure 1. Dimensions of crystallizer at laboratory scale.

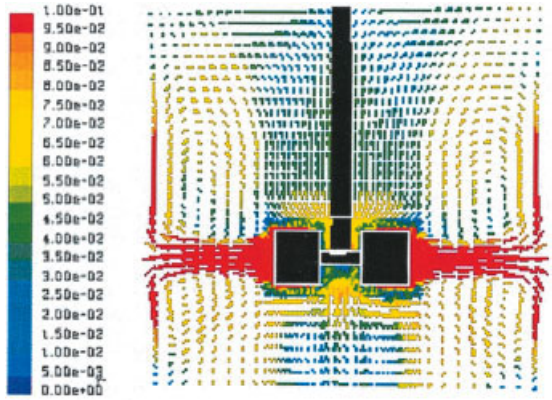

Figure 2. Flow pattern in crystallizer.

Color-scale indicates velocity magnitude in m/s. [Color figure can be viewed in the online issue, which is available at www.interscience.wiley.com.]

CFD simulations are carried out in the absence of solid particles. Mixing at the macroscale is handled with a commercially available software package, Fluent®, which utilizes the finite-volume method to solve the Reynolds-averaged equations of motion with the k-ε model for turbulence. The numerical grid model for the crystallizer is created using the Fluent® utilities Gambit and MixSim.[17]

The simplest types of stirred-tank crystallizer and impeller, with geometry determined by optimal design,[18] are used. The geometric parameters of the stirred tank and impeller are: $d = D/3$, $n_p = 2$, $H = D$, $h = D/3$. The laboratory-scale tank with a volume of 21.2 L is shown in Figure 1. Table 1 lists the crystallizer dimensions and the total volume of ethanol being added (5% of original volume of liquid in the crystallizer).

The flow domain is discretized into 58,610 computational cells for laboratory-scale, 68,205 cells for pilot-plant scale, and 13,3082 cells for industrial-scale crystallizers. With these grid sizes, grid-independent solutions are obtained. In all three models, except for the impeller zone, which consists of mixed-type cells, the remaining sections contain hexahedral cells, which introduce less numerical diffusion errors than tetrahedral cells.

The Fluent® 6.2.16 solver[17] is used to solve the Reynolds-averaged equations of motion together with the standard k-ε turbulence model. A rotation reference frame in which the impeller is at rest, and the tank rotates in the opposite direction is utilized.

As an antisolvent ethanol is continuously fed to the vessel, the governing equations are solved in their transient form. The distribution of ethanol in the vessel is given by the solution of the species transport equation. The feed pipe is not physically present in the numerical grid. In order to simulate the addition of antisolvent, we specify the mass and momentum source in the cell corresponding to the feeding location.[17] Because the amount of antisolvent fed to the vessel is small (5% of the original liquid volume), the volume increase due to antisolvent feeding is neglected. This is equivalent to assuming that antisolvent and water are transported at the same speed inside the reactor. The concentration field of the antisolvent reflects the mixing of antisolvent and primary solvent in the crystallizer.

Table 1. Antisolvent Crystallization Dimensions at Different Scales

Scale	Diameter (m)	Height (m)	Volume (m^3)	Feeding Volume (dm^3)
Lab	0.3	0.3	0.0212	1.06
Pilot	0.85	0.85	0.482	24.1
Industrial	1.1	1.1	1.045	52.24

Results and Discussion

Flow

Different impellers generate mixing of different type and degree. Mixing is driven by the impeller-induced flow and its associated turbulence. Mean flow patterns from CFD simulations plotted in Figure 2 demonstrate that the impeller discharges fluid radially, and the mean flow field consists of two regions, a forced vortex region centered on the axis of the cylindrical vessel, and a region of free vortices bounded by the lateral wall of the cylindrical vessel.[18] There is no momentum or passive scalar (for example, solute) transport due to mean flow between the forced and the free vortex regions. However, there is substantial momentum and solute transport by turbulence between these regions, as evidenced by the uniform solute concentration distribution in the crystallizer of interest. The k-ε model for turbulence utilized in this article, although not as sophisticated as more recent turbulent models, for example, DNS[19] and LES[20] models, estimates high-values for turbulent viscosity and diffusivity in the neighborhood of the boundary between the forced and free vortex regions, thus, enabling physically realistic predictions.

Screening DOE for factors affecting mixing

In antisolvent crystallization, the objective is often to suppress sharp antisolvent concentration gradients, that is, obtain uniform concentration distribution. The factors affecting the antisolvent-concentration distribution are: (1) antisolvent feed position, (2) antisolvent feed rate, and (3) agitation rate.

A screening DOE is conducted for the laboratory-scale crystallizer to study the effect of these factors on mixing. The response function is mixing performance, expressed as standard deviation of the antisolvent-concentration distribution throughout the stirred-tank crystallizer. These factors are listed

Table 2. Factor Values for Two-Level Screening DOE

Factor	Unit	+1	−1
A: Feeding Rate	cm^3/s	8.333	2.083
B: Feeding Position, z	m	0.270	0.100
C: Feeding Position, r	m	0.135	0.070
D: Agitation Rate	rps	10	1.667

in Table 2. In the screening DOE, each factor takes two values, a high-level value that is indicated as +1, and a low-level value that is indicated as −1. In the simulations, $500cm^3$ ethanol is fed into $20dm^3$ water in times 60s and 240s, corresponding to feeding rates of $2.083cm^3/s$ and $8.333cm^3/s$, respectively. Different feeding positions are shown as black dots in Figure 1. A two-level, half factorial DOE[21] is implemented for the laboratory stirred-tank crystallizer and shown in Table 3.

Figure 3 shows top views of antisolvent-concentration distribution at four different levels in the cylindrical vessel. These views provide a measure of the macromixing performance, for the various runs of the screening DOE at dimensionless time (real-time normalized with the residence time, V/Q) equal to one, when the same volume fraction of ethanol has been added to vessels in all runs. Again, black dots indicate the feeding location. Run 2 displays best mixing resulting in almost uniform ethanol-concentration distribution, under conditions of slow feeding and fast agitation. Run 7 shows poor mixing, resulting from fast feeding and slow agitation. Notice that in the Run 7 and Run 6, ethanol accumulation centers on the impeller axis.[18] Runs are ranked in terms of mixing performance from high to low as: 2, 3, 5, 1, 8, 4, 6, and 7.

Figure 4, with top views of antisolvent-concentration distribution at four levels in the crystallizer, for Run 2, at different times, shows that the ethanol concentration in Run 2 stays uniform throughout the simulation time.

A log-log plot of the standard deviation of the antisolvent concentration vs. time in Figure 5 shows that at a very early time (10^{-2} s), the mechanism of mixing switches from convection dominated to convection-and-shear dominated and remains as such up to 0.5 s; from this point in time, thereafter, the mechanism of mixing becomes dispersive.

The results of the screening DOE are also shown in Table 3. This particular form indicates the relative importance of the various factors to the response function. In this Table, the smaller the standard deviation of ethanol concentration (stdv), the better the mixing performance. Run 2 and Run 7 have the lowest and highest stdv, hence, the best and worst mixing performance, respectively. In Table 3, Δ is the difference of

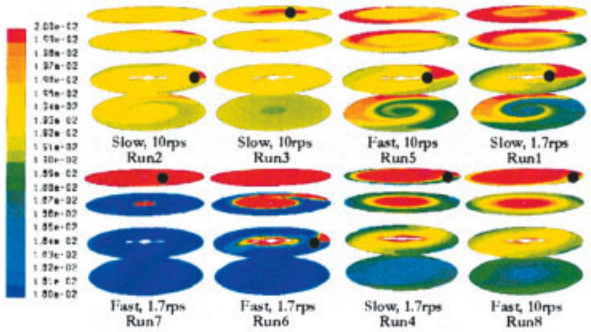

Figure 3. Antisolvent-concentration distribution in the crystallizer for the 8 runs of the screening DOE at dimensionless time equal to one.

[Color figure can be viewed in the online issue, which is available at www.interscience.wiley.com.]

average stdv between high-level and low-level for each factor. By comparing the absolute value of Δ, the various factors are ranked in order of decreasing significance as far as their effect on mixing:

- Agitation rate, D;
- Feeding rate, A;
- Feeding position, z, B;
- Feeding position, r, C.

Agitation rate plays the most important role in mixing, followed by antisolvent feeding rate, and finally, antisolvent feeding position.

Based on the results of the screening DOE, optimal conditions for antisolvent addition for the type of crystallizer in this study call for:

- High-agitation rate;
- Slow-feeding rate;
- Feed position at the same height as the blade;
- Feed position close to the vessel wall.

High-agitation rates and slow-feeding rates ensure uniform distribution of antisolvent throughout the vessel. Since the impeller utilized in the crystallizer models of this work is a radial-flow type, placing the antisolvent feed position in a region at the height of the blade and close to the vessel wall, where both, bulk flow and turbulent energy, are high, results in highly improved micromixing and macromixing.

Table 3. Two-Level, Half-Fractional, Screening DOE

DOE	A	B	C	AB	AC	BC	D	stdv	Index
Run1	−1	−1	−1	+1	+1	+1	−1	0.00100	4
Run2	−1	−1	+1	+1	−1	−1	+1	0.000171	1
Run3	−1	+1	−1	−1	+1	−1	+1	0.000232	2
Run4	−1	+1	+1	−1	−1	+1	−1	0.00170	6
Run5	+1	−1	−1	−1	−1	+1	+1	0.000663	3
Run6	+1	−1	+1	−1	+1	−1	−1	0.00500	7
Run7	+1	+1	−1	+1	−1	−1	−1	0.0363	8
Run8	+1	+1	+1	+1	+1	+1	+1	0.00110	5
stdv ave(+1)	0.01077	0.009833	0.001993	0.009643	0.001833	0.001116	0.0005414		
stdv ave(−1)	0.0007757	0.001708	0.009549	0.001899	0.009708	0.01043	0.01100		
Δ	0.009990	0.008125	−0.007556	0.007744	−0.007875	−0.009310	−0.01046		
	2	3	4				1		

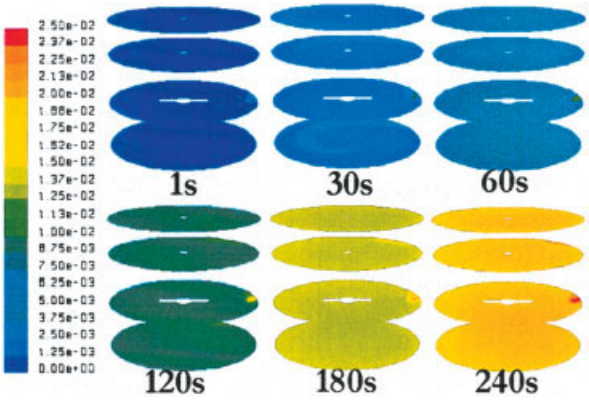

Figure 4. Antisolvent distribution in the crystallizer at different times for Run 2.

[Color figure can be viewed in the online issue, which is available at www.interscience.wiley.com.]

Scale-up by optimization DOE

Once the conditions for optimizing mixing performance in antisolvent crystallization are determined, it is desirable to scale-up mixing performance from laboratory-scale to industrial-scale crystallizers. To this end, an optimization DOE of the Box-Behnken type[21] is designed. The response function is again mixing performance, measured by the spatial uniformity of the antisolvent distribution. For the simulations of the optimization DOE, the feeding position is fixed at its optimal location, point A in Figure 1. The factors in the optimization DOE, then, are: (1) the volume of the crystallizer V, (2) the agitation rate N, and (3) the dimensionless parameter NV/Q, where Q is the antisolvent feeding rate in m^3/s. The consideration behind this choice is to avoid unrealistic combinations of antisolvent feeding rates and crystallizer volumes. Also, NV/Q can be considered as the ratio of the impeller tip speed to antisolvent linear feed rate, $(Nd)/(Q/D^2)$. The factor settings in the optimization DOE at three levels, high, middle, low or -1, 0, $+1$, are displayed in Table 4.

A total of 13 simulations in accordance with Box-Behnken design, are shown in Table 5. The last column in Table 5 is the standard deviation of the ethanol concentration distribution (stdv). The simulations are ranked in terms of mixing performance from high to low as: 4, 6, 1, 5, 9, 3, 7, 2, 8, 10, 13, 12, and 11. Run 4, 9, 3 and 12 are for laboratory- scale, Run 6, 1, 7, 10 and 13 are for pilot-plant-scale, and Run 5, 2, 8, and 11 are for industrial-scale crystallizers.

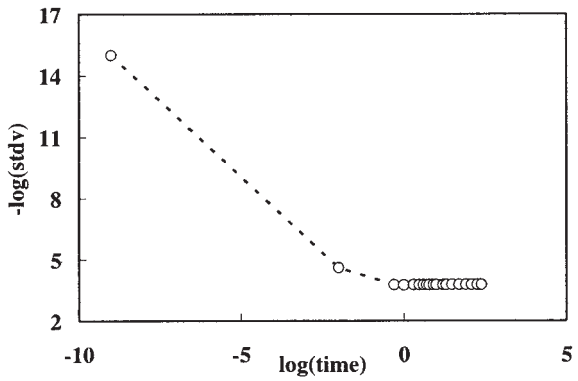

Figure 5. Standard deviation of antisolvent concentration vs. time.

Table 4. Factor Values for Three-Level Optimization DOE

	−1	0	+1
A: Volume, V/m^3	0.0212	0.482	1.045
B: Agitation Rate, N/rps	1.667	5.833	10
C: NV/Q	4375	54688	105000

The total amount of ethanol added in all 13 simulations as percentage of the initial water volume in the vessel is the same. Figure 6 shows antisolvent concentration distribution in the cylindrical vessel with the best and the worst mixing at the industrial scale.

From the results of the DOE, using multiple regression analysis, a statistical correlation of the standard deviation of the antisolvent concentration, *stdv*, in terms of the three factors, N, V and NV/Q is generated. In this correlation, the coefficient of NV/Q is determined with statistical significance greater than 99%, while the coefficients for N and V, insignificant in magnitude when compared to the former, are determined with statistical significance less than 60%. Thus, the correlation resulting from multiple regression analysis can be condensed into

$$10^4 \times stdv = 29.9676 - 0.0008 \times \left(\frac{NV}{Q}\right) \qquad (1)$$

suggesting that mixing performance can be correlated with NV/Q with statistical significance greater than 99%. The expression in (1) confirms that slow antisolvent feeding and high-agitation rate can reduce *stdv* and improve mixing.

Alternatively, systems 1 and 2 can have the similar mixing performance, provided that the dimensionless parameter NV/Q has the same value for both

$$\left(\frac{NV}{Q}\right)_1 = \left(\frac{NV}{Q}\right)_2 \qquad (2)$$

Run 5 in Figure 6 shows good mixing performance in a full scale crystallizer, and meets the scaling criterion of Eq. 2.

Table 5. Box-Behnken Optimization DOE

A	B	C		$10^4 \times$ stdv
0	−1	+1	Run1	1.3565
+1	−1	0	Run2	3.5471
−1	−1	0	Run3	2.3021
−1	0	+1	Run4	1.1496
+1	0	+1	Run5	1.7384
0	+1	+1	Run6	1.2742
0	0	0	Run7	2.4576
0	0	0	Run7	2.4576
0	0	0	Run7	2.4576
+1	+1	0	Run8	3.6383
−1	+1	0	Run9	2.2282
0	−1	−1	Run10	28
+1	0	−1	Run11	45
−1	0	−1	Run12	30
0	+1	−1	Run13	28

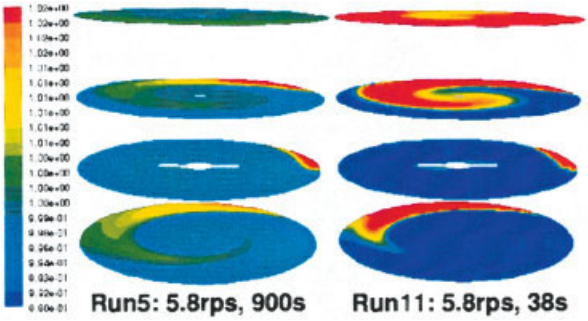

Figure 6. Antisolvent concentration distribution in industrial crystallizers.

[Color figure can be viewed in the online issue, which is available at www.interscience.wiley.com.]

Two other scale-up criteria for crystallizers have been suggested over the years:

- Constant impeller tip speed,
- Constant power input per unit volume.

These criteria have been found in crystallizers where crystallization has significantly progressed.

The scale-up criterion of Eq. 2 is derived from simulations in the absence of crystals. When we attempt to correlate the mixing performance (*stdv*) with the impeller tip speed, the power input per unit volume, and our dimensionless paramete $NV^{1/3}$, $NV^{2/9}$, and *NV*/*Q*, respectively, we find that the *stdv* correlates again with *NV*/*Q* only with statistical significance higher than 99%; the other factors show a weak statistical correlation. Not surprisingly, the scale-up rules, constant impeller tip speed and constant power input per unit volume, cannot ensure mixing similarity for antisolvent and solvent mixtures, since they have been proposed for liquid-particle systems. Mixing in the liquid-particle systems in antisolvent crystallization is the subject of a follow-up study of ours.

Conclusions

A commercially available CFD software package is used to simulate antisolvent crystallization and study the effects of agitation rate, and antisolvent feed rate and position on mixing. The simulations are viewed as numerical experiments that can be designed by DOE methodologies.

Based on a two-level screening DOE, the importance of the various factors, and their optimal settings to achieve uniform mixing of antisolvent and solvent are determined. The settings of the various factors for optimum mixing performance are found to be: (1) higher agitation rate, (2) slower antisolvent feed rate, and (3) Antisolvent feeding position at the same height as blade and close to the wall.

Based on a three-level optimization DOE, a rule for scale-up from laboratory-scale to industrial-scale crystallizers in terms of solvent-antisolvent mixing similarity is found to be centered on the dimensionless parameter *NV*/*Q*, where *N* is the agitation rate, *V* is the volume of the fluid in the vessel, and *Q* is the antisolvent feeding rate.

The mixing studied in this work is limited to single-phase liquid systems. In a follow-up work, we study the effects of various parameters on mixing in liquid-particle systems.

Acknowledgment

The authors are grateful for the financial support provided by the Particle Technology and Crystallization Center.

Notation

d = impeller diameter, m
D = reactor diameter, m
h = the distance between impeller and reactor bottom, m
H = crystallizer height, m
n_p = number of blades
N = agitation speed, rps
Q = antisolvent feed rate, m3/s
stdv = standard deviation of antisolvent distribution
V = reactor volume, m^3

Literature Cited

1. Myerson A. Handbook of industrial crystallization (2nd edition). Butterworth Heinemann; 2002.
2. Mullin JW. Crystallization (4th edition). Butterworth Heinemann, 2001.
3. Zauner R, Jones A. Scale-up of continuous and semibatch precipitation processes. *Ind & Eng Chem Res*. 2000;39:2392-2403.
4. Genck W. Optimizing crystallizer scale up. *Chem Eng Prog*. 2003; 99:36-44.
5. Paul EL, Atiemo-Obeng V, Kresta SM. *Handbook of industrial mixing: science and practice*. NewYork: John Wiley & Sons, Inc.; 2003.
6. Paul EL, Tung HH, Midler M. Organic crystallization processes. *Powder Technol*. 2005;150:133-143.
7. Zauner R, Jones A. On the influence of mixing on crystal precipitation processes-application of the segregated feed model. *Chem Eng Sci*. 2002;57:821-831.
8. Arastoopour H. Numerical simulation and experimental analysis of gas/solid flow systems. *Powder Technol*. 2001;119:59-67.
9. Hatziavramidis D, Sun B, Gidaspow D. Gas-liquid flow through horizontal tees of branching and impacting type. *AIChE J*. 1997;43:1675-1683.
10. Wei H, Garside J. Application of CFD modeling to precipitation system. *Trans IChemE*. 1997;75(A): 219-227.
11. Van Leeuwen MLJ, Bruinsma OSL, Van Rosmalen GM. Influence of mixing on the product quality in precipitation. *Chem Eng Sci*. 1996; 51:2595-2600.
12. Jaworski Z, Nienow A. CFD modeling of continuous precipitation of barium sulphate in a stirred tank. *Chem Eng Sci*. 2003;91:167-174.
13. Wei H, Zhou W, Garside J. Computational fluid dynamics modeling of the precipitation process in a semibatch crystallizer. *Ind & Eng Chem Res*. 2001;40:5255-5261.
14. Fitchett DE, Tarbell JM. Effect of mixing on the precipitation of barium sulphate in an MSMPR reactor. *AIChE J*. 1990;36:511-522.
15. Uehara-Nagamine E, Armenante PM. Effect of process variables on the single-feed semibatch precipitation of barium sulphate. *Trans IChemE*. 2001; 79(A): 979-988.
16. Zauner R, Jones AG. Mixing effects on product particle characteristics from semibatch crystal precipitation. *Trans IChemE*. 2000;78(A):894-902.
17. FLUENT 6.2 User's Guide. NH: Fluent, Inc., 2005.
18. Nagata S. Mixing: principles and applications. NewYork: Wiley; 1975.
19. Moin P, Mahesh K. Direct numerical simulation: a tool in turbulence research. *Annu Rev Fluid Mech*. 1998;30:539-578.
20. Lesieur M, Metais O, Comte P. Large-eddy simulations of turbulence. Cambridge University Press; 2005.
21. Schmidt S, Launsby R. Understanding industrial design experiments. 4th ed. Air Academy Press; 1997.

Manuscript received Dec. 14, 2005, and revision received Jun. 29, 2006.